Spectroscopic and Quartz Crystal Microbalance (QCM) Characterization of Protein-based MIPs

Hazim F. EL-Sharif[1], Hidenbou Aizawa[2], Subrayal M. Reddy[1*]

[1]Department of Chemistry, Faculty of Engineering and Physical Sciences, University of Surrey, Guildford, Surrey, GU2 7XH, UK

[2]Institute for Environmental Management Technology, National Institute of Advanced Industrial Science and Technology (AIST), 1-1 Higashi, Tsukuba 305-8565, Japan

***Corresponding Author**

Tel : +44 (0) 1483686396, **s.reddy@surrey.ac.uk**

Abstract

We have studied acrylamide-based polymers of varying hydrophobicity (acrylamide, AA; N-hydroxymethylacrylamide, NHMA; N-isopropylacrylamide, NiPAm) for their capability of imprinting protein. Rebinding capacities (Q) from spectroscopic studies were highest for bovine haemoglobin (BHb) MIPs based on AA, Q = 4.8 ± 0.21 < NHMA, Q = 4.3 ± 0.32 < NiPAm, Q = 3.6 ± 0.45, while also demonstrating low selectivities for non-template proteins (<30 ± 5%), with the exception of bovine serum albumin (BSA, >76 ± 0.5%). When applied to the QCM sensor as thin-film MIPs, NHMA MIPs were found to exhibit best discrimination between MIP and non-imprinted control polymer (NIP) in the order of NiPAm < AA <

NHMA. The extent of template removal and rebinding, using both crystal impedance and frequency measurements, demonstrated that 10% (w/v):10% (v/v) sodium dodecyl sulphate:acetic acid (pH 2.8) was efficient at eluting template BHb (with 80 ± 10% removal). Selectivity studies of NHMA BHb-MIPs revealed higher adsorption and selective recognition properties to BHb (64.5 kDa) when compared to non-cognate BSA (66 kDa), myoglobin (Mb, 17.5 kDa), lysozyme (Lyz, 14.7 kDa) thaumatin (Thau, 22 kDa) and trypsin (Tryp, 22.3 kDa). The QCM gave frequency shifts of ~1500 ± 50 Hz for template BHb rebinding in both AA and NHMA MIPs, whereas AA-based MIPs exhibited an interference signal of ~2200 ± 50 Hz for non-cognate BSA in comparison to a ~500 ± 50 Hz shift with NHMA MIPs. Our results show that NHMA-based hydrogel MIP are superior to AA and NIPAM..

Keywords: Molecular imprinted polymer (MIP); Hydrogel; Protein; Biosensor; QCM

1. Introduction

1. Introduction

In recent years, molecularly imprinted polymers (MIPs) have allowed selective extractions that rival immunoaffinity-based separations, and have shown clear advantages over real antibodies for sensor applications: they are easy to fabricate, intrinsically stable, robust, and are able to operate in extreme environments [1], [2] and [3]. MIPs could provide an alternative, inexpensive, fast, and efficient diagnostic method for highly sensitive analytical procedures within the pharmaceutical area [3].

When imprinting complex bio-macromolecules some of the most significant drawbacks in MIP technology are the unprecedented degree of influence that the variation in pH [4], ionic strength and local matrix effects all have on the gel properties [5], [6], [7] and [8]. This can affect the three dimensional shape and chemical characteristics of the template molecule during polymerisation. This is particularly true when imprinting large bio-macromolecules such as proteins. Proteins are relatively labile, and have variable conformations which are sensitive to solvent environments, pH and temperature, all of which present a variety of challenges [5]. It has been thought that low imprinting capacities associated with bio-macromolecules could be caused by the use of charged functional monomers causing non-specific electrostatic interactions [5]. Moreover, as with antibodies, MIPs have also shown a degree of cross-selectivity, in that they can bind molecules similar to the native template and cause non-specific binding. It is thought that this is due in part to an excess of functional monomer molecules being randomly distributed and frozen within the imprinted cavity during polymerisation that have an affinity for non-template molecules [3] and [9]. Thus, more sophisticated monomers capable of forming better, stronger and more stable

interactions that offer better positioning and complementary functionality are widely being sought. Once these parameters are optimised, application to biosensors and analysis of actual biological samples would be more realistic [6], [10], [11] and [12].

Biosensors for proteins are currently expensive to develop because they require the use of expensive antibodies [3] and [13]. However, as MIPs are becoming more and more promising as viable alternatives to natural receptors new MIP-based sensor strategies are being developed [3]. The main advantage of biosensors is the ability to sample outside the laboratory environment with minimal user input. One important part of bio-sensing is transducers, which monitor the reaction between bio-selector and analyte. Among various physical transducers (electrochemical, peizoelectric, etc.), mass sensitive devices such as surface acoustic wave (SAW), surface plasmon resonance (SPR) and quartz crystal microbalance (QCM) have become popular for sensing applications [14], [15], [16] and [17].

Following the thorough analysis of QCM systems for use in fluids over the past 2 decades, this has allowed for more esoteric applications including bio-sensing [16]. In most cases quartz resonators are integrated to oscillator circuits to form a QCM for micro weighing applications. Normally, an equivalent circuit model is fitted to the impedance curve, and the obtained parameters can be used for calculating the resonant frequency and dissipation (D) of the quartz crystal i.e. mass and viscoelastic properties of the deposited layers [15] and [16]. Determining the impedance curve has many advantages; first and foremost it has expanded the range of measurable parameters from rigid thin films, to biologically relevant films of "soft" viscoelastic material. These QCM couplings have been widely used for biomaterials and biosensor studies [10], [12], [16], [18] and [19], where surface confined bio-molecular

interactions have provided an insight into dissolution of polymer coatings, DNA hybridisation, cell response to pharmacological substances, molecular interactions of drugs and their delivery. The QCM has also been utilised as an immunosensor, where analytes are recognised by antibodies, which are immobilised on a thin layer deposed on a crystal surface. Resulting mass changes are transformed into an electronically measurable quantity. The objective behind the majority of QCM research is to use sensor technology to develop a rapid method for the measurement of bio-molecular affinity reactions, and an in-depth analysis of electrochemical deposition, adsorption and reaction mechanisms of polymers coated on electrodes as 'thin films' [10], [12], [18], [19] and [20].

The focus of this paper is the tailoring of QCM electrode surface chemistry (i.e. specialised polymer coatings), with a view that these devices can discriminate proteins for bio-sensing and basic surface-molecular interaction studies. In this work, we demonstrate the application of the QCM technique to distinguish between the behaviour of MIPs and NIPs in the presence of cognate and non-cognate proteins. Bovine haemoglobin (BHb, 64.5 kDa) was chosen as a model protein for its well-known function in the vascular system as a carrier of oxygen, also in aiding the transport of carbon dioxide and regulating blood pH [3] and [13]. Bovine serum albumin (BSA, 66 kDa), a non metalloprotein of similar molecular weight to BHb, served to test the selectivity of the BHb-MIP to BSA compared to template BHb, and was compared across a family of acrylamide-based polymer hydrogels.

2. Experimental

2.1. Materials

Acrylamide (AA), N-hydroxymethylacrylamide (NHMA), N-iso-propylacrylamide (NiPAm), N,N′-methylenebisacrylamide (bis-AA), ammonium persulphate (APS), N,N,N′,N′-tetramethylethylenediamine (TEMED), sodium dodecyl-sulphate (SDS), glacial acetic acid (AcOH), bovine haemoglobin (BHb), bovine serum albumin (BSA), hen egg-white lysozyme (Lyz), thaumatin from Thaumatococcus danielii (Thau), bovine pancreatic trypsin (Tryp) and equine heart myoglobin (Mb) were all purchased from Sigma–Aldrich, Poole, Dorset, UK. Sieves (75 μm) were purchased from Endecotts Ltd. and Inoxia Ltd., UK. AT-cut quartz crystal pieces (9 MHz fundamental resonance) with gold-on-chrome electrodes were supplied by Nihon Dempa Kogyo Company Ltd. (Tokyo, Japan).

2.2. HydroMIP preparations

Hydrogel MIPs were synthesised by separately dissolving AA (54 mg), NHMA (77 mg), NiPAm (85.6 mg) and bis-AA as cross-linker (6 mg), (8.5 mg) and (9.5 mg), respectively along with template protein (12 mg) in 960 μL of MilliQ water. The solutions were purged with nitrogen for 5 min, followed by an addition of 20 μL of a 10% (w/v) APS solution and 20 μL of a 5% (v/v) TEMED solution. Polymerisation occurred at room temperature (RT, 22 ± 2 °C) giving total gel densities (%T) of 6%T, AA/bis-AA (w/v); 8.5%T, NHMA/bis-AA (w/v); 9.5%T, NiPAm/bis-AA (w/v), and final crosslinking densities (%C) of 10%C (9:1, w/w) for all hydrogels.

For every MIP created a non-imprinted control polymer (NIP) was prepared in an identical manner but in the absence of protein. After polymerisation, the gels were granulated separately using a 75 μm sieve. Of the resulting gels, 500 mg were transferred into 1.5 mL centrifuge Eppendorf tubes and conditioned by washing with five 1 mL volumes of MilliQ water followed by five 1 mL volumes of 10% (w/v):10% (v/v) SDS:AcOH (pH 2.8) and another five 1 mL volume washes of MilliQ water to remove any residual 10% (w/v):10% (v/v) SDS:AcOH eluent and equilibrated the gels. Each wash step was followed by a centrifugation, whereby the gels were centrifuged using an Eppendorf mini-spin plus centrifuge for 3 min at 6000 rpm (RCF: 2419 × g). All supernatants were collected for analysis by spectrophotometry to verify the extent of template removal. It should be noted that the last water wash and eluent fractions were not observed to contain any protein. Therefore we are confident that any remaining template protein within the MIPs did not continue to leach out during the rebinding studies.

2.3. Rebinding studies

Once the gels (500 mg) were equilibrated, a 1 mL template protein solution prepared in MilliQ water containing 3 mg of protein was added to the target MIPs and NIP controls and was allowed to associate at RT (22 ± 2 °C) for 20 min. Selectivity studies were also conducted to assess the relative imprinting factor of the original protein template. This was achieved by loading non-cognate proteins on a BHb imprinted gel. Gels were then washed with four 1 mL volumes of MilliQ water. Each reload and wash step for all MIPs and NIP controls was followed by centrifugation at 6000 rpm (RCF: 2419 × g) for 3 min. All supernatants were collected for analysis by spectrophotometry.

2.4. Spectrophotometric analysis

Calibration curves in MilliQ water and 10% (w/v):10% (v/v) SDS:AcOH were prepared for BHb, BSA, Lyz, Tryp and Mb. Spectral scans revealed peak wavelengths for BHb in MilliQ water and 10% (w/v):10% (v/v) SDS:AcOH to be 405 nm and 395 nm, respectively. Peak wavelengths for BSA in MilliQ water and 10% (w/v):10% (v/v) SDS:AcOH were found to be 288 nm and 290 nm respectively. Peak wavelengths for Lyz in MilliQ water and 10% AcOH:SDS were found to be 291 nm and 296 nm respectively. Peak wavelengths for Tryp in MilliQ water and 10% (w/v):10% (v/v) SDS:AcOH were found to be 293 nm. Peak wavelengths for Mb in MilliQ water, 10% (w/v):10% (v/v) SDS:AcOH were found to be 410 nm, and 396 nm respectively. Analysis and subsequent determination of protein concentration in appropriate media was performed at specific peak wavelengths using a UV mini-1240 CE spectrophotometer (Shimadzu Europa, Milton Keynes, UK).

2.5. Quartz crystal microbalance (QCM) analysis of thin film MIPs

QCM crystals were sealed and air capped (single-sided) with PVC glue in-order to prevent short circuiting when the QCM was submerged in solution [10]. Poly AA, NHMA and NiPAm gels for BHb were synthesised using the hydrogel production procedures outlined in Section 2.2. Before polymerisation, MIPs and NIPs were deposited as thin films onto the capped QCM crystals. Thin-films were achieved by beading and compressing 10 μL of the polymerising solutions directly onto the crystals. QCM frequency and impedance

175 measurements were taken using an Agilent 4194A Impedance Analyser. An in-house written
176 QBasic programme was used to drive the analyser and collect series resonance frequency and
177 impedance data in real time.

178

179 2.5.1. Elution and rebinding studies

180

181 MIP and NIP polyAA thin-film capped crystals were firstly immersed in MilliQ water,
182 followed by 10% (w/v):10% (v/v) SDS:AcOH in order to remove imprinted protein primarily
183 from the surface of the polymer. This was followed by another submersion in MilliQ water to
184 remove any residual surfactant and to re-condition the hydrogel. After subsequent
185 stabilisation of the QCM response, template protein was reloaded by immersing the QCM in
186 a 3 mg/mL BHb solution and the response trace was recorded at RT (22 ± 2 °C).

187

188 2.5.2. Selectivity studies

189

190 Continuous real-time scans were conducted in-order to assess characteristic impedance
191 changes of the gels during surface exposure to wash, elute and protein rebinding conditions.
192 During a typical run, the MIP thin-film capped crystals were submerged sequentially in
193 various solutions such as 10% (w/v):10% (v/v) SDS:AcOH, MilliQ water or 3 mg/mL protein
194 solutions (cognate BHb and non-cognate BSA, Thau, Lyz and Tryp) for a set time of 5 min
195 each, and crystal impedance and frequency responses were recorded at RT (22 ± 2 °C). The
196 latter procedure was followed for AA, NiPAm and NHMA based MIP hydrogels for BHb.

197

198 3. Results and discussion

199 3.1. MIP selectivity

200 The molecular imprinting effect is characterised by the rebinding capacity (Q) of protein to
201 the gel polymer (mg/g) exhibited by the protein-specific MIP and the control NIP, and is
202 calculated using Eq. (1), where Ci and Cr are the initial protein and the recovered protein
203 concentrations (mg/mL) respectively (which specifies the specific protein bound within the
204 gel), V is the volume of the initial solution (mL), and g is the mass of the gel polymers (g).

205

206 $$Q = \frac{[C_i - C_r]V}{g} \quad (1)$$

207

208 Fig. 1A shows the rebinding capacities and imprinting factors of polyacrylamide (polyAA)
209 MIP and NIPs for several different proteins. The internal measure of the imprinting factor
210 between MIP and NIP serves to demonstrate that the MIP possesses selective cavities for the
211 rebinding of template molecule compared to NIP controls. It can clearly be seen that there is
212 a distinctive rebinding capacity variation for each imprinted protein template within a
213 polyAA MIP. This has previously been attributed to protein size, cross-linking density, and
214 the initial degree of association within the polymer matrix [4].

215 Gels based on N-hydroxymethylacrylamide (NHMA) exhibited similar rebinding trends,
216 whereas poly-N-isopropylacrylamide gels (polyNiPAm) demonstrated lower rebinding
217 capacities. Thus, bulk gel characterisation revealed the highest rebinding capacities for BHb
218 MIPs based on polyAA (Q = 4.8 ± 0.21), followed by polyNHMA (Q = 4.3 ± 0.32),

polyNiPAm (Q = 3.6 ± 0.45). These gel imprinting trends are in agreement with those previously published [4], [9] and [10].

Selectivity studies were also conducted to confirm a BHb specific imprinting effect and to assess the relative imprinting factor of cross-selective binding profiles. The cross-reactivity of the BHb-imprinted MIPs for non-cognate proteins was quantified using relative imprinting factors (k), Eq. (2), where IFBHb is the imprinting factor for BHb, and is calculated by IF = [Ci − Cr]MIP/[Ci − Cr]NIP, and IFx is the imprinting factor of the cross-reacting non-cognate proteins on a BHb MIP. For the template BHb k = 1, and for non-cognate proteins that are less-specific for the BHb MIP, k < 1.

$$k = \frac{\mathrm{IF}_{BHb}}{\mathrm{IF}_{x}} \qquad (2)$$

The data (Fig. 1B) suggests that both non-cognate trypsin (Tryp) and lysozyme (Lyz) proteins have relatively low affinities for the BHb-specific MIP, k ≈0.2 ± 0.05. However, bovine serum albumin (BSA), which is a similar size to BHb, exhibited a high degree of interference binding (cross selectivity) resulting in high k values of 0.65 ± 0.05. Myoglobin (Mb) also exhibited some degree of cross-selectivity; this can be attributed to the size of Mb, which is a quarter that of BHb (17.5 kDa), and its similarity to a single BHb sub-unit [4]. Interestingly though, when reversed, a polyAA BSA-MIP exposed to non-target BHb protein had relatively low affinity. It would appear that BSA has a high ability to bind non-specifically to a BHb MIP, whereas BHb does not exhibit the same ability within a BSA MIP.

Competitive binding studies using a 50:50 mixture of BHb:BSA (3 mg/mL total) on a MIP-BHb were also conducted (Fig. 1B). The addition of BSA caused an obvious capacity decrease of BHb binding on the BHb-MIP, suggesting that the rebinding of BHb was displaced by the competing BSA or by protein-protein interactions [21]. As the size, structure, and specificity of the imprinted cavities should be in favour of the BHb template, it is rational that the addition of BSA as a competing protein would not bind to the BHb-specific imprinted cavities. Gai et al. previously demonstrated that BSA does not bind specifically to a BHb MIP, but rather displaces the non-specific recognition sites of cavities and the nonspecific binding of BHb to BHb-MIP [21]. Moreover, although BSA and BHb share similar sizes (66 kDa and 64.5 kDa, respectively), it should be noted that BSA has a pI of 4.6 and BHb a pI of (6.8–7.0). Since competitive binding was performed under MilliQ water (pH 5.4), conditions are in favour of BSA [21] and [22]. Above its pI, BSA becomes negatively charged and the groups exist as single bondNH2 and single bondCOO−, this overall negative net charge induces more favourable and complementary hydrogen bonding interactions, resulting in increased specific as well as non-specific binding [4].

3.2. QCM sensor application of MIPs

Thin film BHb MIPs were prepared on the surface of a QCM chip and the sensor was exposed sequentially to MilliQ water, 10% (w/v):10% (v/v) SDS:AcOH and 3 mg/mL protein solutions at RT (22 ± 2 °C). We have previously published on the thickness of the thin films on sensor chips with an average thickness of 138 ± 9 nm [6]. Given that for a 9 MHz crystal the shear wave decay length is 250 nm at RT [23], we are within the sensing region of the QCM to measure both bulk and surface effects within the MIP film.

Fig. 2A and B shows the QCM impedance and frequency responses following immersion in a solution of 10% (w/v):10% (v/v) SDS:AcOH in order to remove imprinted protein from the surface of the polymer. Previous investigations have shown that optimum conditions for protein removal of up to 80% have been achieved using 10% (w/v):10% (v/v) SDS:AcOH [9]. Using this acid/surfactant combination the positively charged protein attaches to the negatively charged surface of SDS micelles and disrupts the hydrophobic bonds. Since there is a significant shift in both resonance frequency and impedance it can be assumed that some of the BHb imprinted template has been successfully removed from the MIP.

It is worth noting the two distinct differences in the impedance response when compared with the frequency response. Firstly, the impedance response has much reduced noise in the signal in contrast to the frequency response. Secondly, there are significant additional transitions (e.g. at 350 and 650 s) in the signal which are being observed in the Z response, but not in the frequency response. It has been suggested that whereas the frequency response predominately demonstrates the QCM mass response only within an adlayer, the electrical impedance gives a combination response of the mass effect as well as subsequent changes in the viscoelasticity of the adlayer possibly due to molecular relaxations within the adsorbed layer over a longer timescale following initial immersion [23], [24] and [25].

After subsequent stabilisation of the QCM response, the template BHb was then reloaded by immersing the QCM in a 3 mg/mL BHb solution and the response trace recorded. Fig. 2C and D compares the final QCM impedance and frequency responses to template BHb exposure of each MIP and its corresponding NIP. It can be seen that upon addition of a 3 mg/mL BHb solution to the BHb MIP caused significant QCM responses compared with NIP thin-film hydrogels. This suggests that MIP thin-film gels are affected by specific binding of target

BHb. This distinct difference between responses exhibited by MIP and the NIP control strongly supports that binding and elution of target protein gave rise to distinct impedance transitions. The 200 ± 50 Hz frequency shift observable by both MIP and NIP during the initial loading step (Fig. 2D) is suggestive of a solution viscosity effect.

Real time impedance response following sequential immersion in solutions of BHb, 10% (w/v):10% (v/v) SDS:AcOH and BSA were also measured. Three distinct types of responses were observed depending on the acrylamide-based monomer used. The key difference between the polymers is their hydrophilicity dictated by the hydrophilic hydroxyl group in NHMA and the hydrophobic isopropyl group in NiPAm. AA sits between the two in degree of hydrophilicity (polyNHMA > polyAA > polyNiPAm), which agrees with the order of best performance of the polymers as BHb MIPs in previous QCM studies [10]. Fig. 3 compares the final QCM response to cognate and non-cognate protein exposure of each MIP with its corresponding NIP. Interestingly, the NiPAm MIP and NIP both show a near zero frequency response to template BHb and non-cognate BSA, indicating that NiPAm is equally unselective for both proteins as is the control non-imprinted polymer. The non-response of NiPAm to either BHb or BSA suggests that there is a resistance to either protein to bind to the polymer. The striking difference in selectivities between cognate and non-cognate proteins for NHMA and AA suggests that the hydroxyl group in NHMA plays a significant role in the selective binding of BHb and the lack of binding of BSA.

Moreover, variations of the series resonance frequency demonstrated to be highly dependent on the test solution used (Fig. 4A). The impedance data is presented here because in comparison to the frequency response, there is much reduced noise in the signal following each solution phase immersion. It can be seen that MIP thin-films exposed to a 10%:10%

(v/v) SDS:AcOH solution exhibited an immediate significant decrease in impedance (500 ± 100 Ω); this is possibly due to the increase in the viscosity of the solution caused by the presence of SDS micelles in the solution. Moreover, it can clearly be seen that the introduction of non-template BSA also exhibits an impedance response within the poly AA MIP, suggesting some non-specific binding within the BHb-HydroMIP. Thus, there is a high degree of cross-selectivity present for our AA-based MIPs (>70%), and this interference is absent when NHMA-based MIPs are used (<20%) as seen in Fig. 3.

To further test the BHb-MIP selectivity, we investigated the rebinding of template BHb after exposing the MIP with non-target BSA. The resulting quantified imprinting effect of BHb for polyAA MIP thin-film gels can be seen in the impedance responses (Fig. 4B). The comparison demonstrates that both HydroMIP and HydroNIP films act differently under water wash, elution and load (solution immersion) treatments following BSA loading. It can be seen that when non-target BSA is loaded first, the QCM impedance response is now negligible. Interestingly, impedance responses are also almost negligible when BHb is introduced after prior exposure to BSA. Although the loaded BSA did not associate specifically with the BHb-MIP thin-film surface, an interesting and lasting effect inhibits BHb from easily binding to recognition sites. Indeed, BSA is similar to the template BHb in size, but the spatial arrangement of the effective groups on its exterior are different from BHb, and the recognition sites in the BHb-MIP cavities are not complementary in shape to BSA [22]. Therefore, little to no selectivity of BSA on BHb-MIPs should be expected. Therefore, in the case of AA-based MIPs, the inhibition effect is most likely due to the ability of BSA to exhibit protein binding on the MIP surface but not within cavities. Formation of a BSA biolayer above (but not within) the cavities would block subsequent cavity-selective MIP binding for its cognate protein [22]. This is further indication that BHb-MIPs distinguish proteins not only based on molecular size, but also on the synergistic effect of shape memory,

and multiple weak hydrogen bonding interactions specific to template protein in macromolecular recognition [21], [22] and [26].

Moreover, further studies to interrogate the recognition capabilities of MIPs were carried out using a range of non-metalloproteins chosen for their different sizes and functionalities compared to BHb, BSA and Mb. Of these proteins: lysozyme (Lyz), a glycoside hydrolase enzyme (14.7 kDa) that is part of the innate immune system, and exists as a natural form of protection from pathogens like Salmonella, E. coli, and Pseudomonas [9], [10] and [27]. Thaumatin (Thau), a sweetener or flavour modifier (22 kDa) often used in crystallisation studies due to its ease of use and crystal formation [27]. Trypsin (Tryp), a serine protease enzyme or proteinase 'digestive enzyme' (23.8 kDa) commonly imprinted within MIPs [9], [10] and [27]. Fig. 5 shows that the BHb-MIPs based on all three polymers (AA, NHMA, and NiPAm) are essentially non-responsive to the addition of the three smaller proteins Thau, Lyz and Tryp respectively. An average NIP response was calculated based on all three polymers and used as an illustration to demonstrate the negligible responses exhibited by the MIP properties. The negligible responses exhibited by the QCM sensor concur with the qualitative data and confirm that these small proteins exhibit no selective specific/non-specific binding characteristics to a BHb-imprinted MIP.

4. Conclusions

A family of acrylamide-based MIPs have been characterised for their imprint efficiency using spectrophotometric and QCM sensor techniques for biosensor development. Varied rebinding capacities and relative imprinting factors have been achieved using bulk characterisation. We

have demonstrated that MIP selectivity is a function of the hydrophilicity of the acrylamide monomer used to form the MIP. Three distinct types of QCM responses were observed depending on the acrylamide used (polyNHMA > polyAA > polyNiPAm), which agrees with the order of best performance of the polymers in previously published QCM studies. The selectivity of BHb-MIP for BHb and BSA was also compared via QCM, along with several other proteins. Results demonstrated BHb-MIP to have better selective adsorption and recognition properties to BHb than BSA when using the hydrophilic NHMA as a MIP polymer matrix. Therefore, the QCM sensor was able to indicate MIP surface activity and provide physical interpretation in terms of hydrophilicity of the polymer matrix that forms the MIP and protein selectivity. Our QCM sensor also has the ability to assess the extent of specific protein binding by sensing surface-specific bound cognate protein to MIPs compared to non-imprint NIP controls. We expect, once fully developed, that the benefits of sensitivity, specificity and stability of MIPs coupled with discriminatory techniques, such as QCM, will be crucial to the future impact of portable diagnostics for personal healthcare and use by health professionals. The technology also presents major potential benefits to environmental and food monitoring.

Acknowledgements

The authors wish to thank the UK Engineering and Physical Sciences Research Council (EPSRC) Grants (EP/G014299/1) and NERC/ACTF (RSC) for supporting this work.

References

[1] S. Pradhan, M. Boopathi, O. Kumar, A. Baghel, P. Pandey, T.H. Mahato, B. Singh, R. Vijayaraghavan, Molecularly imprinted nanopatterns for the recognition of biological warfare agent ricin Biosens. Bioelectron., 25 (2009), pp. 592–598

[2] D.R. Kryscio, N.A. Peppas Critical review and perspective of macromolecularly imprinted polymers Acta Biomater., 8 (2012), pp. 461–473

[3] M.J. Whitcombe, I. Chianella, L. Larcombe, S.A. Piletsky, J. Noble, R. Porter, A. Horgan The rational development of molecularly imprinted polymer-based sensors for protein detection Chem. Soc. Rev., 40 (2011), pp. 1547–1571

[4]H.F. El-Sharif, Q.T. Phan, S.M. Reddy Enhanced selectivity of hydrogel-based molecularly imprinted polymers (HydroMIPs) following buffer conditioning Anal. Chim. Acta, 809 (2014), pp. 155–161

[5] E. Verheyen, J.P. Schillemans, M. van Wijk, M. Demeniex, W.E. Hennink, C.F. van Nostrum Challenges for the effective molecular imprinting of proteins Biomaterials, 32 (2011), pp. 3008–3020

[6] S.M. Reddy, D.M. Hawkins, Q.T. Phan, D. Stevenson, K. Warriner Protein detection using hydrogel-based molecularly imprinted polymers integrated with dual polarisation interferometry Sens. Actuators B: Chem., 176 (2013), pp. 190–197

[7] S.A. Piletsky, N.W. Turner, P. Laitenberger Molecularly imprinted polymers in clinical diagnostics – future potential and existing problems Med. Eng. Phys., 28 (2006), pp. 971–977

[8] M.E. Byrne, V. Salian Molecular imprinting within hydrogels. II. Progress and analysis of the field Int. J. Pharm., 364 (2008), pp. 188–212

405 [9] D.M. Hawkins, D. Stevenson, S.M. Reddy Investigation of protein imprinting in
406 hydrogel-based molecularly imprinted polymers (HydroMIPs) Anal. Chim. Acta, 542 (2005),
407 pp. 61–65

408

409 [10] S.M. Reddy, Q.T. Phan, H. El-Sharif, L. Govada, D. Stevenson, N.E. Chayen

410 Protein crystallization and biosensor applications of hydrogel-based molecularly imprinted
411 polymers Biomacromolecules, 13 (2012), pp. 3959–3965

412 [11] P.A. Lieberzeit, R. Samardzic, K. Kotova, M. Hussain MIP sensors on the way to
413 biotech application: selectivity and ruggedness Proc. Eng., 47 (2012), pp. 534–537

414 [12] B.B. Prasad, I. Pandey Molecularly imprinted polymer-based piezoelectric sensor for
415 enantio-selective analysis of malic acid isomers Sens. Actuators B: Chem., 181 (2013), pp.
416 596–604

417 [13]S.M. Reddy, G. Sette, Q. Phan Electrochemical probing of selective haemoglobin
418 binding in hydrogel-based molecularly imprinted polymersElectrochim. Acta, 56 (2011), pp.
419 9203–9208

420 [14]G.N.M. Ferreira, A. da-Silva, B. Tomé Acoustic wave biosensors: physical models and
421 biological applications of quartz crystal microbalance Trends Biotechnol., 27 (2009), pp.
422 689–697

423 [15] T.M.A. Gronewold Surface acoustic wave sensors in the bioanalytical field: recent
424 trends and challenges Anal. Chim. Acta, 603 (2007), pp. 119–128

425

426 [16] U. Latif, S. Can, O. Hayden, P. Grillberger, F.L. Dickert Sauerbrey and anti-Sauerbrey
427 behavioral studies in QCM sensors – detection of bioanalytes Sens. Actuators B: Chem., 176
428 (2013), pp. 825–830

429 [17]C. Steinem, A. Janshoff Sensors: piezoelectric resonators P. Worsfold, A. Townshend,
430 C. Poole (Eds.), Encyclopedia of Analytical Science (2nd ed.), Elsevier, Oxford (2005), pp.
431 269–276

432 [18] K.K. Reddy, K.V. Gobi Artificial molecular recognition material based biosensor for
433 creatinine by electrochemical impedance analysis Sens. Actuators B: Chem., 183 (2013), pp.
434 356–363.

435 [19] K. Reimhult, K. Yoshimatsu, K. Risveden, S. Chen, L. Ye, A. Krozer
436 Characterization of QCM sensor surfaces coated with molecularly imprinted nanoparticles
437 Biosens. Bioelectron., 23 (2008), pp. 1908–1914

438 [20] B. Khadro, C. Sanglar, A. Bonhomme, A. Errachid, N. Jaffrezic-Renault
439 Molecularly imprinted polymers (MIP) based electrochemical sensor for detection of urea
440 and creatinine Proc. Eng., 5 (2010), pp. 371–374

441 [21] Q. Gai, F. Qu, T. Zhang, Y. Zhang The preparation of bovine serum albumin surface-
442 imprinted superparamagnetic polymer with the assistance of basic functional monomer its
443 application for protein separation J. Chromatogr. A, 1218 (2011), pp. 3489–3495

444 [22] Q. Gai, F. Qu, Y. ZhangThe preparation of BHb-molecularly imprinted gel polymers
445 and its selectivity comparison to BHb and BSA Sep. Sci. Technol., 45 (2010), pp. 2394–2399

446

View Record in Scopus | Full Text via CrossRef | Citing articles (9)

[23]K.A. Marx Quartz crystal microbalance: a useful tool for studying thin polymer films and complex biomolecular systems at the solution–surface interface

Biomacromolecules, 4 (2003), pp. 1099–1120

[24] S. Kurosawa, J. Park, H. Aizawa, S. Wakida, H. Tao, K. Ishihara Quartz crystal microbalance immunosensors for environmental monitoring Biosens. Bioelectron., 22 (2006), pp. 473–481

[25] T. Zhou, K.A. Marx, M. Warren, H. Schulze, S.J. Braunhut

The quartz crystal microbalance as a continuous monitoring tool for the study of endothelial cell surface attachment and growth Biotechnol. Prog., 16 (2000), pp. 268–277

[26] Zhou Xue, He Xi-Wen, Chen Lang-Xing, Li Wen-You, Zhang Yu-Kui

Optimum conditions of separation selectivity based on molecularly imprinted polymers of bovine serum albumin formed on surface of aminosilica Chin. J. Anal. Chem., 37 (2009), pp. 174–180

[27] E. Saridakis, S. Khurshid, L. Govada, Q. Phan, D. Hawkins, G.V. Crichlow, E. Lolis, S.M. Reddy, N.E. Chayen Protein crystallization facilitated by molecularly imprinted polymers Proc. Natl. Acad. Sci., 108 (2011), pp. 11081–11086

Fig. 1.

(A) Rebinding capacities (*Q*) and imprinting factors of MIP_{polyAA} and NIP_{polyAA} hydrogels for several proteins in MilliQ water media: bovine haemoglobin (BHb), bovine serum albumin (BSA), myoglobin (Mb), lysozyme (Lyz), trypsin (Tryp); (B) relative imprinting factors (*k*) for a range of BHb-MIP_{polyAA} cross-reactants in MilliQ water media. Results illustrate higher MIP selectivities for cognate BHb and the degree of cross-selectivity for other non-template analytes. Data represents mean ± S.E.M., *n* = 3.

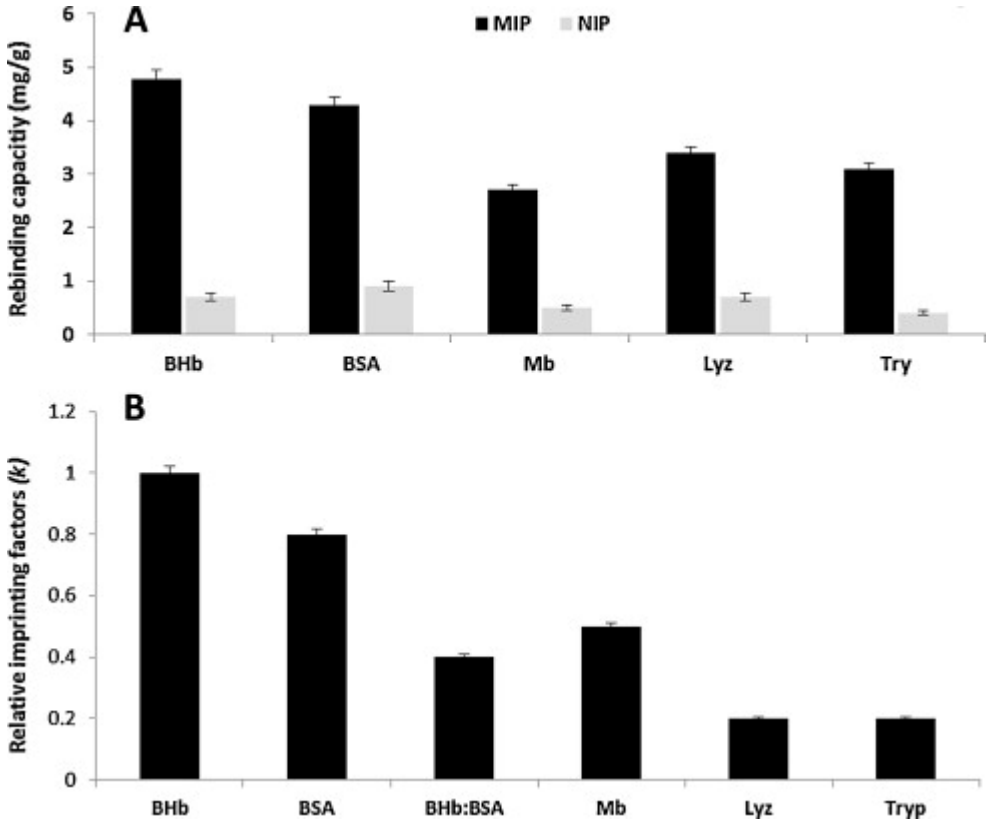

Fig. 2.

QCM response to the immersion of polyAA-BHb hydrogel thin-film MIP in 10% (w/v):10% (v/v) SDS:AcOH in order to follow protein elution (arrow indicates time of MIP immersion): (A) impedance (Δ*Z*), (B) frequency (Δf); QCM responses to BHb (3 mg/mL) loading onto a BHb imprinted polyAA hydrogel thin-film (arrow indicates time of immersion in protein solution): (C) impedance (Δ*Z*) and (D) frequency (Δ*f*).

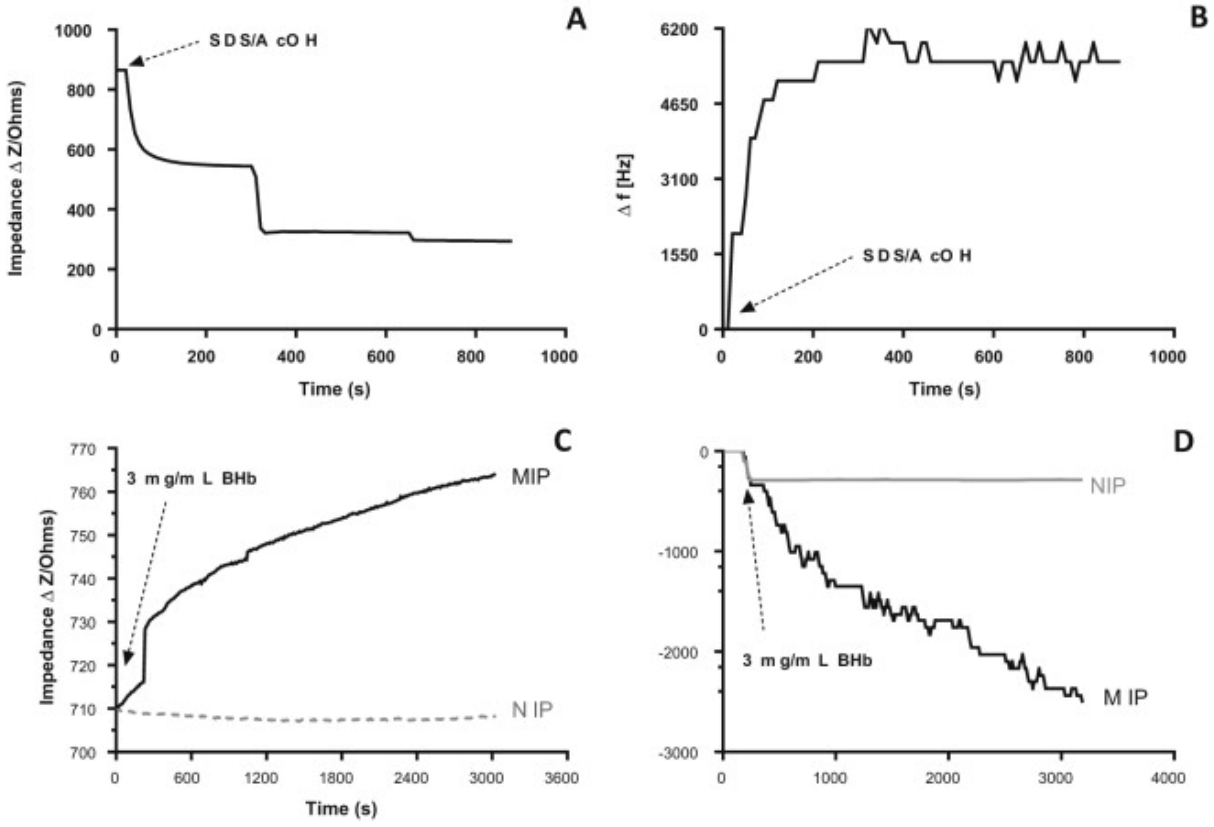

481

482

483 Fig. 3.

484 QCM frequency shift responses of NiPAm, AA and NHMA polymer MIPs and NIPs to cognate BHb
485 and non-cognate BSA loading (3 mg/mL) after 5 min of exposure. Data represents
486 mean ± S.E.M., *n* = 3.

487

488

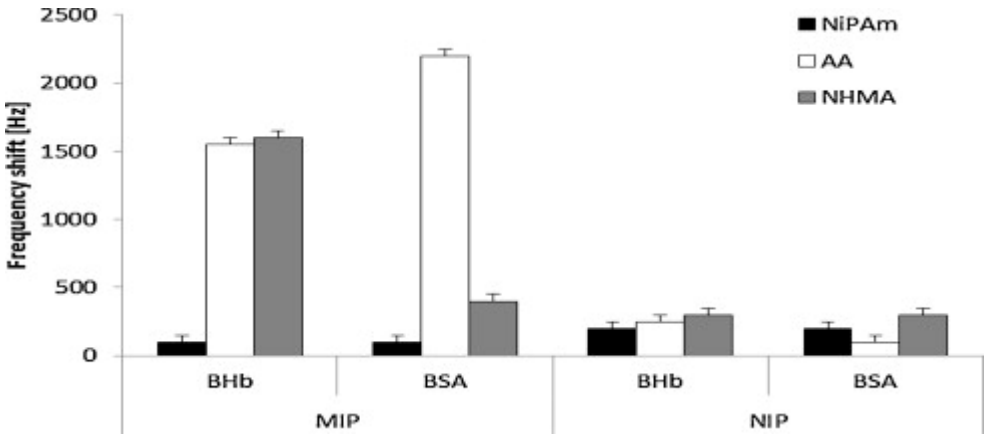

489

490 Fig. 4.

491 Real time QCM impedance responses: (A) direct BHb rebinding and BSA cross-selectivity on a BHb-
492 MIP_{polyAA}; (B) BSA cross-selectivity on a BHb-MIP_{polyAA} followed by BHb rebinding.

493

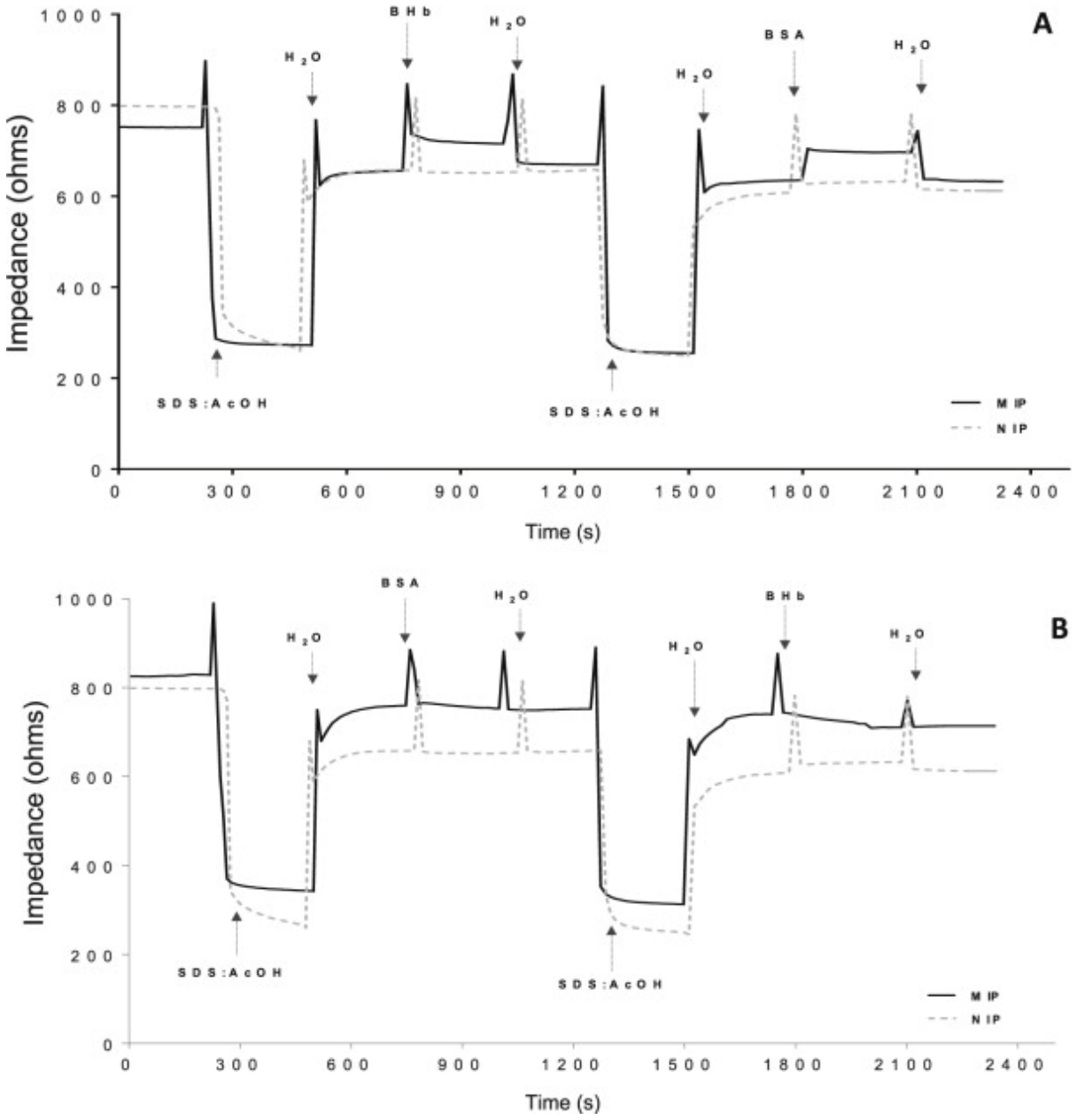

494

495

496 Fig. 5.

497 QCM response of functionalised acrylamide BHb MIPs to non-cognate proteins thaumatin (Thau),

498 lysozyme (Lyz), and trypsin (Tryp) after H_2O washes and an SDS:AcOH elute.

499

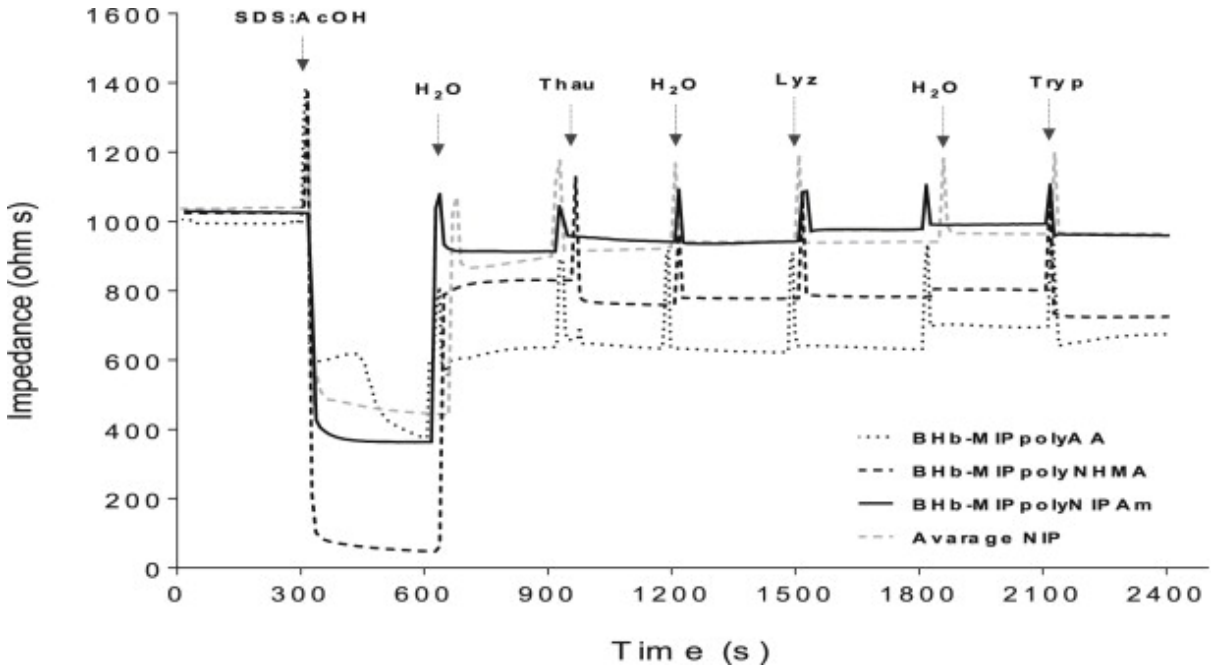

500

501

502

503

504

505

506

507

508